

# Carbon membrane gas separation of binary CO<sub>2</sub> mixtures at high pressure

*N. Kruse*<sup>a</sup>, *Y. Schießler*<sup>a</sup>, *S. Kämnitz*<sup>b</sup>, *H. Richter*<sup>b</sup>, *I. Voigt*<sup>b</sup>, *G. Braun*<sup>a</sup>, *J. U. Repke*<sup>c</sup>

<sup>a</sup> TH Köln, <sup>b</sup> Fraunhofer IKTS, <sup>c</sup> TU Bergakademie Freiberg

## Abstract

The key feature of inorganic membranes is the ability to operate at high temperature and pressure. Even supercritical solvents can be processed by these membranes, whereas polymer membranes tend to swell and consequently suffer from reduced selectivity and mechanical strength. The combination of chemical and mechanical stability of ceramic membranes opens completely new fields of applications, e.g. in membrane reactors for chemical reactions like H<sub>2</sub>-synthesis by dehydrogenation. This work investigates the selectivity and permeance of carbon membranes for binary mixtures composed of Helium, Nitrogen, Oxygen or Carbon dioxide in a pressure region up to 20 MPa and a temperature range from 300 to 450 K. A Maxwell-Stefan diffusion approach has been applied to study the gas to gas and gas to membrane interactions under high pressure condition.

## 1. Introduction

The separation of gas mixtures employing inorganic membranes is an established part of the current membrane research activities. One reason for investigating the performance of these membranes is their excellent selectivity and permeability compared to other recent membrane types [1]. Another reason is their capability to operate at high temperature and high pressure. For polymer membranes successful operation at higher pressure is reported as well [2]. However, high fugacities of components that are well soluble in the membrane material leads to plasticization [3] and therefore to serious reduction in mechanical strength. Since it is thermodynamically impossible to increase the fugacity of one component from feed to permeate side a high transmembrane pressure, compared to the feed pressure, is required to achieve an increase of concentration and a decrease of fugacity from feed to permeate side at the same time. Therefore mechanical strength is necessary to separate mixtures of small molecules without using sweep gas. In comparison to polymer membranes, the mechanical strength of carbon based membranes is not affected by sorption which makes them predestined for operation at high transmembrane pressure.

Despite their potential applicability to high pressure gas separation, very limited research has been carried out on this topic. As far as we know, less than a half dozen of articles has been published in journals on gas separation with carbon membranes at pressures

above 2 MPa [1,4–7] and none at pressures above 10 MPa.

For modelling gas transport through carbon membranes, many approaches have been published as summarised by Ismail and David [8]. Obviously, size exclusion (molecular sieving) and adsorption phenomena play a significant role for the selective transport through the membrane. Both factors can be taken into account by using Fick's law and deriving the local concentrations from the adsorption isotherms. This has been shown for example by J. E. Koresh and A. Soffer [9]. For higher pressures this attempt is not practical because the Fick diffusivity coefficients become strongly dependent on the local concentrations of all components.

Therefore, the more general approach of Maxwell–Stefan diffusion has to be applied, which is better suited to deal with the fluid to membrane and fluid to fluid interactions. Krishna [10,11] proposed the following implementation for binary mixtures in zeolites and other crystalline materials:

$$\begin{aligned} -\frac{\rho q_1}{RT} \cdot \nabla \mu_1 &= \frac{x_2 \cdot j_1 - x_1 \cdot j_2}{D_{12}} + \frac{j_1}{D_1} \\ -\frac{\rho q_2}{RT} \cdot \nabla \mu_2 &= \frac{x_1 \cdot j_2 - x_2 \cdot j_1}{D_{12}} + \frac{j_2}{D_2} \end{aligned} \quad \text{Eq. 1}$$

Where  $\rho q$  is the volumetric adsorption,  $R$  the universal gas constant,  $T$  the temperature,  $\mu$  the chemical potential,  $x$  the molar fraction in the adsorbate phase,  $j$  the molar flux and  $D$  the Maxwell–Stefan diffusion

coefficient for gas to gas and gas to membrane interactions. Assuming no temperature gradients in the separation layer the chemical potential can be described by the fugacity  $f$ :

$$d\mu = RT \frac{1}{f} df \quad \text{Eq. 2}$$

For estimating the adsorption equilibrium of two mixture components in the membrane, a modified Langmuir isotherm described by Markham and Benton [12] can be applied (Eq. 3). The model takes into account the competing adsorption as seen in the following equation, where  $q_s$  is the saturation loading,  $b$  the Langmuir-coefficient and  $f$  the fugacity:

$$q_1 = \frac{q_{s,1} f_1 b_1}{1 + f_1 b_1 + f_2 b_2} \quad \text{Eq. 3}$$

This theoretical approach combined with mixed gas permeance measurements should contribute to a better understanding of the mass transport in carbon membranes at high pressure to advance membrane technology into new industrial applications.

## 2. Experimental

### 2.1 Membrane

The tested membrane type has a tubular configuration with an inner diameter of 7 mm, outer diameter of 10 mm and a total length of 250 mm. The carbon separation layer is placed on the inside wall of a porous aluminium oxide ceramic tube and has a thickness of 2  $\mu\text{m}$ . Multiple intermediate layers ensure a smooth interface between separation layer and support tube (Fig. 1). The effective membrane area is  $5.3 \cdot 10^{-3} \text{ m}^2$  and the pore size of the separation layer is below 0.5 nm. A maximum mechanical strength of 9.2 MPa transmembrane pressure was determined. The membrane has been developed and manufactured by Fraunhofer IKTS/Hermsdorf. A comprehensive and detailed overview on carbon membrane fabrication is given by S.M. Saufi and A.F. Ismail [13].

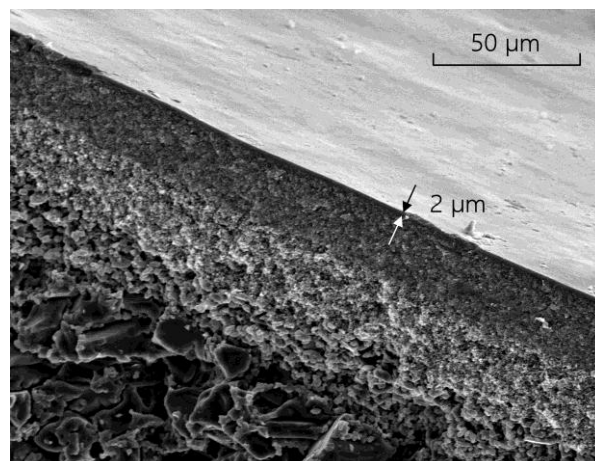


Fig. 1: SEM image showing the cross section of the carbon separation layer, the intermediate layers and the support tube

### 2.2 Membrane cell

To investigate the membrane behaviour, a specialized high pressure membrane cell has been developed and built (Fig. 2). Besides mechanical strength and temperature resistance, the different thermal expansion coefficients of steel and the membrane material were considered. Therefore, the membrane is mounted to retainer elements which are freely movable in axial direction to prevent thermal strain on the membrane. Furthermore, the sealing cross section of the retainer elements are dimensioned in such a manner that transmembrane pressure does not cause any axial force on the membrane. All machined parts are made from stainless steel. Sealing is implemented by FKM O-rings.

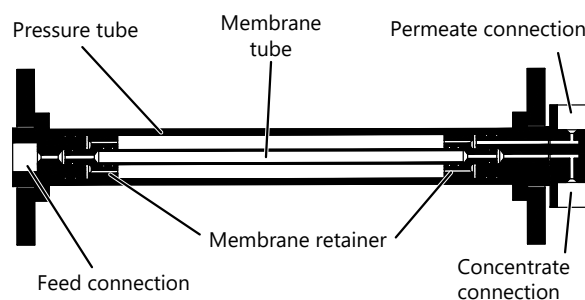


Fig. 2: High pressure membrane test cell

### 2.3 Experimental plant

For this research a high pressure test plant (Fig. 3) has been designed. The plant is capable of conducting measurements with pressures up to 20 MPa. Feed and permeate pressure can be controlled independently. The possible operating temperature ranges from 300 to 450 K.

Feed gas components are supplied by 30 MPa cylinders or by a cooled high pressure pump for fluids with low vapour pressure (e.g. CO<sub>2</sub>, propane, butane). A real time capable PLC controls pressures, retentate flow rate and feed composition as well as the cell temperature. Moreover, the PLC ensures that the strain on the membrane is kept below its maximum strength during pressure changes.

Pneumatic valves on the feed, retentate and permeate sides of the module allow a fast control of pressures and flows. The feed side valve between gas cylinder and membrane controls the feed pressure by a PID loop. On the permeate side a feedback controlled valve between the membrane module and ambient pressure ensures the desired permeate pressure.

The retentate flow is measured by a coriolis flow meter and the permeate flow by a thermal flow meter. Both are manufactured by Bronkhorst High-Tech. To derive molar flows, the thermal capacity flow signal, measured by the thermal flow meter, is combined with data from an online composition measurement system.

The online composition measurement system utilizes thermal conductivity sensors in the permeate and retentate stream. The method described by Wassiljewa, Mason and Saxena [14] is used to determine the thermal conductivity of binary mixtures. It is solved numerically on the PLC to derive the compositions from the measured thermal conductivities in real time. The online composition data allows a feed-back-control of

perature is better than 2 K. Composition measuring accuracy depends significantly on the difference in heat conductivity of the two components. For the investigated mixtures the accuracy of the composition difference between permeate and retentate is better than  $\pm 1\%$ . Permeate flow rate is measured with a relative accuracy between  $\pm 1\%$  and  $\pm 4\%$  depending on the absolute flow.

## 2.4 Measurements

All measuring points for further investigation were taken at steady state. For single gas measurements pressure change and reaching the steady state takes less than a minute. For mixtures it takes significantly longer to reach stable conditions. At low permeate flow rates and high permeate pressures, it takes up to 20 minutes to achieve a steady state condition on the permeate side. The online concentration measurement allows observation of gradients over time and therefore a reliable identification of steady state.

For each measuring point temperature, feed pressure, permeate pressure, retentate flow and feed concentration are fixed. The difference between feed and permeate pressure (transmembrane pressure) does not exceed 7 MPa for all measurements to prevent mechanical failure of the membrane support tube. The retentate flow rate is chosen in such a way that the composition changes only insignificantly from feed to retentate side. Therefore, the retentate flow rate is con-

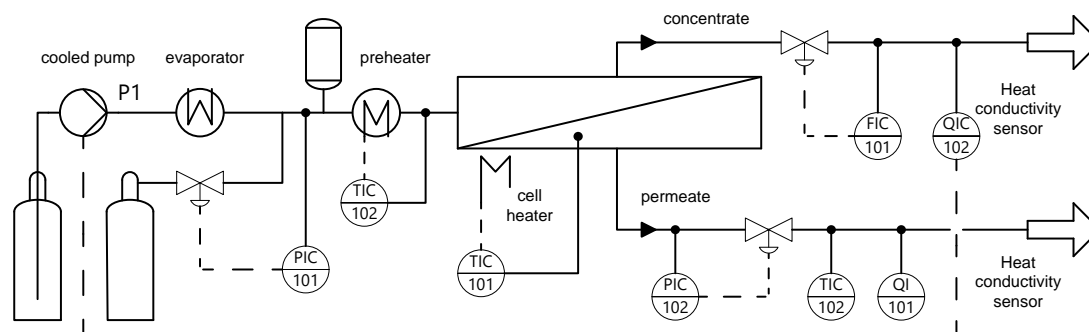


Fig. 3: Set-up of the high pressure experimental membrane plant

the feed pump to set the specified feed composition.

To guarantee the desired temperature inside the membrane module, the test plant controls multiple electric heat sources. One heater evaporates the liquid fluid stream from the high pressure pump before it is mixed with the second component from the gas cylinder. This mixture is then preheated to the temperature of the membrane test cell. A third heater keeps the test cell temperature constant. Measuring accuracy for tem-

perature is better than 2 K. Composition measuring accuracy depends significantly on the difference in heat conductivity of the two components. For the investigated mixtures the accuracy of the composition difference between permeate and retentate is better than  $\pm 1\%$ . Permeate flow rate is measured with a relative accuracy between  $\pm 1\%$  and  $\pm 4\%$  depending on the absolute flow.

Single gas permeance experiments were conducted with He, N<sub>2</sub>, O<sub>2</sub> and CO<sub>2</sub> at up to 20 MPa feed pressure. In order to investigate the membrane selectivity, measurements with equimolar mixtures composed of He and CO<sub>2</sub>, O<sub>2</sub> and CO<sub>2</sub> as well as N<sub>2</sub> and CO<sub>2</sub> have been carried out. The high pressure condition causes significant deviation from ideal gas behaviour. Therefore, the

permeance  $P_i$  is defined by molar flux per fugacity difference between feed and permeate side of the membrane (Eq. 4).

$$P_i = \frac{J_i}{f_{i,f} - f_{i,p}} \quad \text{Eq. 4}$$

The fugacities are determined by integrating equation of state data [15–18]. Selectivities  $S_{ij}$  are determined by the quotient of the measured molar component ratio on feed and permeate side as shown in Eq. 5.

$$S_{ij} = \frac{x_{i,p} / x_{j,p}}{x_{i,f} / x_{j,f}} \quad \text{Eq. 5}$$

As a result of the substantial pressure at the permeate side of the membrane, this expression has a much smaller value than the permeance quotient of both components that is often used as well. Consequently, the number directly represents the technically feasible performance. This relationship between selectivity and pressure on the permeate side has been comprehensively discussed by Huang et al [19].

### 3. Results and discussion

#### 3.1 Single gas permeance

The results show that a pressurisation of an unused membrane up to high pressures causes a persistent reduction of permeance. For  $\text{CO}_2$  the effect is most substantial (Fig. 4). The reduction is more than 90 % between an unused membrane and a membrane after pressurization to 18 MPa (measured at 10 MPa feed pressure and 1 MPa transmembrane pressure for both cases). In the case of He the permeance reduction takes place as well (Fig. 5), but the effect is much smaller. The reduction is less than 25 % at a pressurisation with 14 MPa. While staying below the maximum pressurisation pressure, increasing and decreasing the pressure results in reproducible permeance measurements. It is to note that the absolute permeance numbers from Fig. 4 and Fig. 5 cannot be compared since both measurements took place on an unused and therefore different membrane.

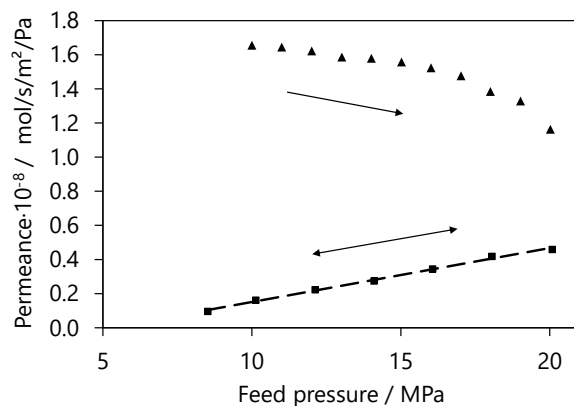


Fig. 4:  $\text{CO}_2$  permeance at 1 MPa transmembrane pressure plotted against the feed pressure for the first pressurization of the unused membrane ( $\blacktriangle$ ) and the reproducible region of the pressurized membrane ( $\blacksquare$ ) at 373 K

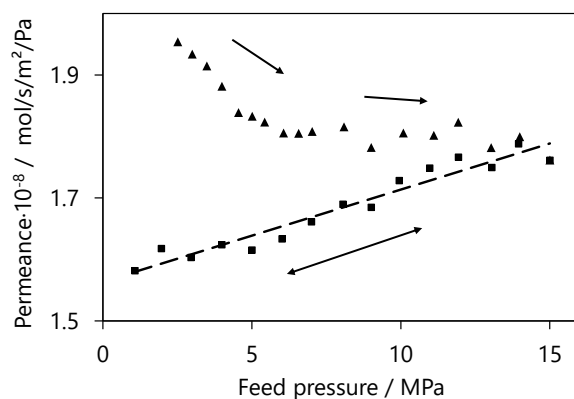


Fig. 5: He permeance at 1 MPa transmembrane pressure plotted against the feed pressure for the first pressurization of the unused membrane ( $\blacktriangle$ ) and the reproducible region of the pressurized membrane ( $\blacksquare$ ) at 300 K

Since this behaviour depends on the feed pressure rather than on the transmembrane pressure (transmembrane pressure has been kept constant at 1 MPa), a mechanical reason like compacting of the separation layer or support structure can be excluded. It can be assumed that the molecules bound to the surface inside the separation layer in an adsorption-like manner. However, in contrast to conventional adsorption phenomena, this effect is not reversible. Lowering the pressure after the first pressurization does not result in a release of the molecules that cause the permeance reduction.

This effect is properly related to changes to the graphite structure itself. Several publications suggest that the gas molecules between the graphene layers cause a significant displacement of the carbon structure. Koresh [20] showed this hysteresis effect by adsorption

measurements at pressures below 100 kPa. Kobayashi et al. [21] studied the properties of carbon fibres and correlated the electric conductivity to the adsorption that caused the swelling. While most publications have investigated activated carbon with high porosity and a significant fraction of mesopores, it is to admit that the membrane material is significant more dense and therefore more ridged. Nevertheless, the measured data indicates that the swelling effect is even for ceramic supported membranes relevant if exposed to very high pressures.

To take this effect into account and ensure reproducible results the membranes of all following measurements were prepared by pressurization to the maximum pressure of that particular measurement with the respective gas or gas mixture.

### 3.2 Binary mixtures

As expected, there are significant differences between the transport of a single gas and a gas in a mixture, especially for high pressures. That becomes quite apparent as shown by the measured fluxes in Fig. 6. While single gas permeation of CO<sub>2</sub> and O<sub>2</sub> strongly diverge with a rising pressure, the behaviour in the mixture seems primary determined by the CO<sub>2</sub> flux.

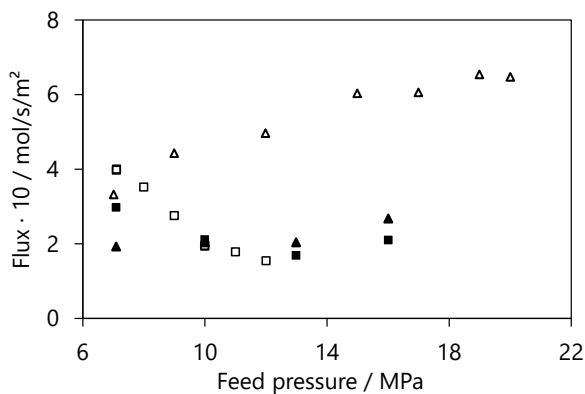


Fig. 6: Flux of CO<sub>2</sub> (□) and O<sub>2</sub> (Δ) as single gases as well as CO<sub>2</sub> (■) and O<sub>2</sub> (▲) in an equimolar mixture at 300 K and a transmembrane pressure of 7 MPa

The results show separation for equimolar CO<sub>2</sub>-mixtures with He and N<sub>2</sub> even for very high pressures (Fig. 7 and Fig. 8). The theoretical maximum selectivity, shown in both diagrams, indicates the separation factor where the fugacity of the better permeating CO<sub>2</sub> is equal on feed and permeate side of the membrane by definition of the separation factor (Eq. 5). For separation factors above that limit a transport against the driving

potential (fugacity gradient) would be required and is therefore not possible.

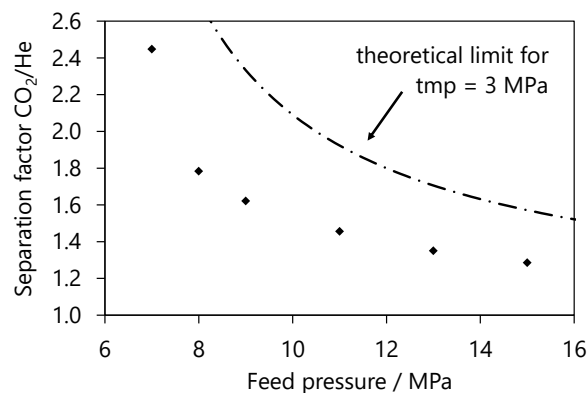


Fig. 7: Dependency of the separation factor on feed pressure for an equimolar CO<sub>2</sub>/He mixture at 3 MPa transmembrane pressure

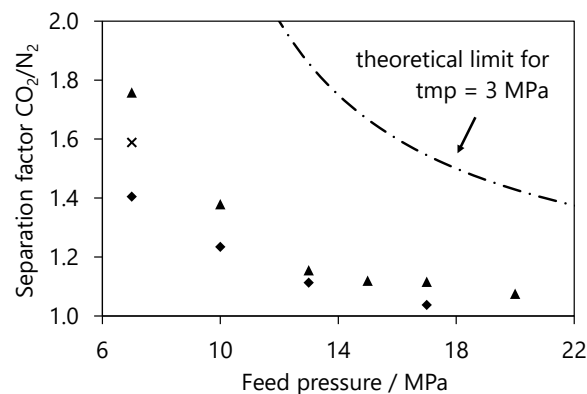


Fig. 8: Dependency of the separation factor on feed pressure for an equimolar CO<sub>2</sub>/N<sub>2</sub> mixture at transmembrane pressure of 3 (♦), 4 (×) and 5 MPa (▲)

At a feed pressure of 11.5 MPa and a transmembrane pressure of 3 MPa a flux of  $6.5 \cdot 10^{-2}$  mol/s/m<sup>2</sup> was determined. As expected, a high transmembrane pressure increases the flux and selectivity of the membrane, whereas high permeate pressure decreases selectivity.

The Maxwell-Stefan diffusion coefficients for an equimolar feed mixture of N<sub>2</sub>/CO<sub>2</sub> have been determined by multivariable regression on the measured multicomponent fluxes. Therefore, the system of differential equations shown in Eq. 1 has been numerical integrated over the separation layer thickness. It has to take into account that many commonly applied simplifications are not valid for high adsorption loadings, so that an analytic solution was not achievable. The Nelder–Mead method [22] has been used for minimizing the differences between measured und calculated

values to approximate the diffusion coefficients. The adsorption has been modelled as shown in Eq. 3 with parameters determined from our high pressure gravimetric adsorption measurements (Fig. 9).

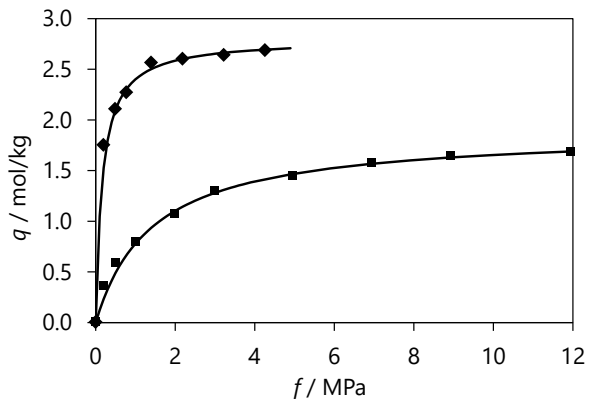


Fig. 9: Single gas sorption isotherms of the carbon membrane material with CO<sub>2</sub> (◆) and N<sub>2</sub> (■) at 300 K and a fugacity range at up to 12 MPa. Lines indicate the corresponding Langmuir model.

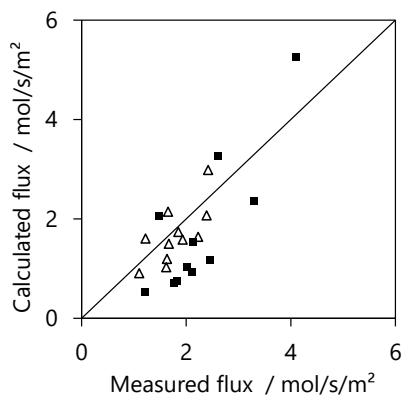


Fig. 10: Comparison of measured and modelled flux data of N<sub>2</sub> (Δ) and CO<sub>2</sub> (■) for an equimolar feed mixture at 7 to 20 MPa at a temperature of 300 K

Even though this model shows a limited accuracy for describing the measured fluxes over the whole pressure range (Fig. 10), the determined Maxwell-Stefan diffusion coefficients give a distinct view on the interactions between the mixture components and the membrane. As shown by the coefficients in Table 1 the transport of N<sub>2</sub> is only determined by the interaction with CO<sub>2</sub>, while the N<sub>2</sub>/membrane interaction is negligible ( $D_1 \gg D_{12}$ ). For CO<sub>2</sub> flux the interactions with N<sub>2</sub> have an impact as well, but the CO<sub>2</sub>/membrane interaction is here substantial.

**Table 1**

Maxwell-Stefan diffusion coefficients

Symbol	$D \cdot 10^{-6} / \text{m}^2/\text{s}$	Description
$D_1$	6150	N <sub>2</sub> / membrane
$D_2$	5.9	CO <sub>2</sub> / membrane
$D_{12}$	17.5	N <sub>2</sub> / CO <sub>2</sub>

To investigate the temperature dependence of mass transport, an equimolar CO<sub>2</sub>/N<sub>2</sub>-mixture has been studied between 300 and 450 K (7 MPa feed pressure and 0.1 MPa on the permeate side). The extensive temperature span shows (Fig. 11) that the transmembrane flux of CO<sub>2</sub> and N<sub>2</sub> can be described by an Arrhenius type equation ( $j = j_0 \cdot \exp(-E_A/RT)$ ).

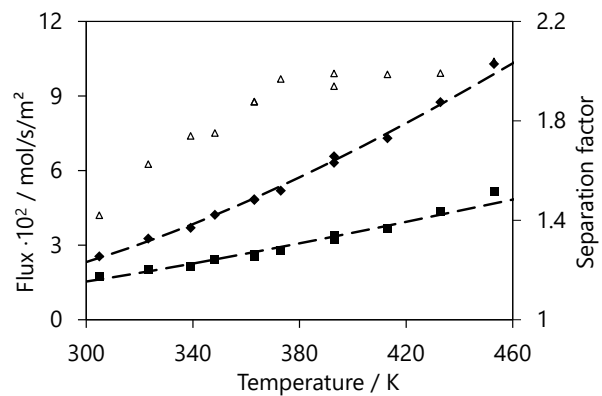


Fig. 11: Dependency of membrane flux on temperature at 7 MPa feed and 0.1 MPa permeate pressure for CO<sub>2</sub> (◆) and N<sub>2</sub> (■) with Arrhenius fit and separation factor (Δ)

The activation energies derived from the Arrhenius analysis in comparison to the measurements of other authors are shown in Table 2. It is noticeable that for most low pressure measurements the temperature dependence for CO<sub>2</sub> is smaller than for N<sub>2</sub>. For high pressure that seems to change thus the selectivity for CO<sub>2</sub> significantly increases with rising temperature in comparison to low pressure CO<sub>2</sub>/N<sub>2</sub>-separation. Fuertes and Centeno suggested that the low temperature dependence of CO<sub>2</sub> permeance at low pressure is a result of a compensation between increasing mobility and decreasing adsorption [23]. For high pressure transport a contribution of multiple temperature dependent effects is expected as well. With rising pressure the absorptivity ratio of CO<sub>2</sub> over N<sub>2</sub> is getting smaller (Fig. 9) and therefore the membrane selectivity seems to become dominated by the difference of the component's mobility.

**Table 2**  
Activation energy  $E_A$  (kJ/mol) for different pressures

$p$ / MPa	CO <sub>2</sub>	N <sub>2</sub>	
7.0	10.7	8.2	this work
0.2	2.4	6.8	[24]
0.1	-4.4	-4.5	[25]
< 0.1	9.2	18.3	[26]
n.a.	0.0	9.8	[23]

## 4. Conclusion

High pressure mixed gas experiments have been carried out to investigate the deployment of carbon membranes for new gas separation applications at up to 20 MPa. A Maxwell-Stefan diffusion approach has been applied to study the gas to gas and gas to membrane interactions at these conditions.

The outcomes of this research show promising results for applying carbon membranes to high pressure and high temperature separation processes. Even for very high pressures reasonable selectivities are achievable. For operation with high pressure on the permeate side a sufficient transmembrane pressure is required to keep a substantial difference of fugacity for the better permeating component between feed and permeate side. Otherwise the selectivity is limited not by the membrane performance itself but by the lack of driving potential.

The Maxwell-Stefan diffusion coefficients acquired from the measured data gives a valuable insight to the interactions of the gases to each other and to the membrane material. While the N<sub>2</sub> transport is dominated by the interaction with CO<sub>2</sub>, the CO<sub>2</sub> transport itself is largely determined by wall interactions. The variations between modelled and measured transport indicates that even after a onetime high pressure exposure the carbon structure itself is not static, which has influence to the transport coefficients.

To take the effect of structural changes of the carbon material at into account, it seems to be beneficial to further investigate these changes with additional methods beside permeance and adsorption measurements.

## 5. References

- [1] R. Swaidan, X. Ma, E. Litwiller, I. Pinnau, High pressure pure- and mixed-gas separation of CO<sub>2</sub>/CH<sub>4</sub> by thermally-rearranged and carbon molecular sieve membranes derived from a polyimide of intrinsic microporosity, *J. Memb. Sci.* 447 (2013) 387–394. doi:10.1016/j.memsci.2013.07.057.
- [2] G. Härtel, Permselectivity of a PA6 membrane for the separation of a compressed CO<sub>2</sub>/H<sub>2</sub> gas mixture at elevated pressures, *J. Memb. Sci.* 162 (1999) 1–8. doi:10.1016/S0376-7388(99)00066-6.
- [3] W. Ogieglo, L. Upadhyaya, M. Wessling, A. Nijmeijer, N.E. Benes, Effects of time, temperature, and pressure in the vicinity of the glass transition of a swollen polymer, *J. Memb. Sci.* 464 (2014) 80–85. doi:10.1016/j.memsci.2014.04.013.
- [4] F.K. Katsaros, T. a. Steriotis, A.K. Stubos, A. Mitropoulos, N.K. Kanellopoulos, S. Tension, High pressure gas permeability of microporous carbon membranes, *Microporous Mater.* 8 (1997) 171–176. doi:10.1016/S0927-6513(96)00080-6.
- [5] F.K. Katsaros, T.A. Steriotis, G.E. Romanos, M. Konstantakou, A.K. Stubos, N.K. Kanellopoulos, Preparation and characterisation of gas selective microporous carbon membranes, *Microporous Mesoporous Mater.* 99 (2007) 181. doi:10.1016/j.micromeso.2006.07.041.
- [6] K. Wang, L.S. Loo, K. Haraya, CO<sub>2</sub> Permeation in Carbon Membranes with Different Degrees of Carbonization, *Ind. Eng. Chem. Res.* 46 (2007) 1402–1407. doi:10.1021/ie060617a.
- [7] E.P. Favvas, Carbon dioxide permeation study through carbon hollow fiber membranes at pressures up to 55bar, *Sep. Purif. Technol.* 134 (2014) 158–162. doi:10.1016/j.seppur.2014.07.041.
- [8] A. ISMAIL, L. DAVID, A review on the latest development of carbon membranes for gas separation, *J. Memb. Sci.* 193 (2001) 1–18. doi:10.1016/S0376-7388(01)00510-5.
- [9] J.E. Koresh, A. Soffer, Mechanism of permeation through molecular-sieve carbon membrane. Part 1. — The effect of adsorption and the dependence on pressure, *J. Chem. Soc. Faraday Trans. 1 Phys. Chem. Condens. Phases.* 82 (1986) 2057. doi:10.1039/f19868202057.
- [10] R. Krishna, The Maxwell–Stefan description of mixture diffusion in nanoporous crystalline materials, *Microporous Mesoporous Mater.* 185 (2014) 30–50. doi:10.1016/j.micromeso.2013.10.026.
- [11] R. Krishna, Describing the diffusion of guest molecules inside porous structures, *J. Phys. Chem. C.* 113 (2009) 19756–19781. doi:10.1021/jp906879d.
- [12] E.C. Markham, A.F. Benton, The Adsorption of Gas Mixtures by Silica, *J. Am. Chem. Soc.* 53 (1931) 497–507. doi:10.1021/ja01353a013.
- [13] S. Saufi, A.F. Ismail, Fabrication of carbon membranes for gas separation—a review, *Carbon N. Y.* 42 (2004) 241–259. doi:10.1016/j.carbon.2003.10.022.
- [14] M.P. Saksena, S.C. Saxena, Thermal conductivity of polyatomic gas mixtures and Wassiljewa form, *Appl. Sci. Res.* 17 (1967) 326–330. doi:10.1007/BF02116434.
- [15] R. Span, W. Wagner, A New Equation of State for Carbon Dioxide Covering the Fluid Region from the Triple-Point Temperature to 1100 K at Pressures up to 800 MPa, *J. Phys. Chem. Ref. Data.* 25 (1996) 1509. doi:10.1063/1.555991.
- [16] R. Span, A Reference Equation of State for the

- Thermodynamic Properties of Nitrogen for Temperatures from 63.151 to 1000 K and Pressures to 2200 MPa, *J. Phys. Chem. Ref. Data.* 29 (2000) 1361. doi:10.1063/1.1349047.
- [17] R.D. Mc Carty, Thermodynamic Properties of Helium 4 from 2 to 1500 K at Pressures to 108 Pa, *J. Phys. Chem. Ref. Data.* 2 (1973) 923. doi:10.1063/1.3253133.
- [18] R.B. Steward, R.T. Jacobsen, W. Wagner, Thermodynamic properties of O<sub>2</sub> from the triple point to 300K with pressures to 80 MPa, *J. Phys. Chem. Ref. Data.* 20 (1991) 917–1021. doi:10.1063/1.555897.
- [19] Y. Huang, T.C. Merkel, R.W. Baker, Pressure ratio and its impact on membrane gas separation processes, *J. Memb. Sci.* 463 (2014) 33–40. doi:10.1016/j.memsci.2014.03.016.
- [20] J.E. Koresh, On the flexibility of the carbon skeleton, *J. Chem. Soc. Faraday Trans.* 89 (1993) 935. doi:10.1039/ft9938900935.
- [21] N. Kobayashi, T. Enoki, C. Ishii, K. Kaneko, M. Endo, Gas adsorption effects on structural and electrical properties of activated carbon fibers, *J. Chem. Phys.* 109 (1998) 1983. doi:10.1063/1.476774.
- [22] J. a. Nelder, R. Mead, A simplex method for function minimization, *Comput. J.* 7 (1964) 308–313. doi:10.1093/comjnl/7.4.308.
- [23] A.B. Fuertes, T.A. Centeno, Preparation of supported asymmetric carbon molecular sieve membranes, *J. Memb. Sci.* 144 (1998) 105–111. doi:10.1016/S0376-7388(98)00037-4.
- [24] X. He, M. Hägg, Hollow fiber carbon membranes: From material to application, *Chem. Eng. J.* 215-216 (2013) 440–448. doi:10.1016/j.cej.2012.10.051.
- [25] K. Briceño, A. Iulianelli, D. Montané, R. Garcia-Valls, A. Basile, Carbon molecular sieve membranes supported on non-modified ceramic tubes for hydrogen separation in membrane reactors, *Int. J. Hydrogen Energy.* 37 (2012) 13536–13544. doi:10.1016/j.ijhydene.2012.06.069.
- [26] E.P. Favvas, E.P. Kouvelos, G.E. Romanos, G.I. Pilatos, a. C. Mitropoulos, N.K. Kanellopoulos, Characterization of highly selective microporous carbon hollow fiber membranes prepared from a commercial co-polyimide precursor, *J. Porous Mater.* 15 (2007) 625–633. doi:10.1007/s10934-007-9142-2.